pH Dependent Thermodynamic and Amide Exchange Studies of the *C*-Terminal Domain of the Ribosomal Protein L9: Implications for Unfolded State Structure†

Ying Li,‡ Jia-Cherng Horng,‡,|| and Daniel P. Raleigh*,‡,§

Department of Chemistry, State University of New York at Stony Brook, Stony Brook, New York 11794-3400, and Graduate Program in Biochemistry and Structural Biology, State University of New York at Stony Brook, Stony Brook, New York 11794

Received December 12, 2005; Revised Manuscript Received February 19, 2006

ABSTRACT: It is now recognized that unfolded states of globular proteins are not random coils but instead can contain significant amounts of residual structure. Here, we combine amide H/D exchange studies and thermodynamic measurements to probe pH dependent structure in the unfolded state of the small, mixed α-β protein CTL9. The *m* value measured by urea denaturation is strongly dependent upon pD, increasing by 40% from pD 7.5 to 4.85. Likewise, the change in heat capacity upon unfolding, $\Delta C_p°$, increases significantly from pD 7.5 to 5.5. These studies argue that the unfolded state contains interactions, presumably hydrophobic in nature, that lead to a more compact state at high pH. The expansion at lower pH correlates with the estimated unfolded state pK_a values of the three histidines in CTL9 with additional contributions from acid side chains at the lower pH. Amide H/D exchange studies were conducted at pD 5.0, 6.0, and 7.0. At pD 5.0, the exchange rates could be measured for 44 residues, 29 of which exchanged by global unfolding. No evidence was found for any super protected sites, that is, sites that exchange at rates slower than those expected for global exchange. The estimated precision for the experiments limits detection to residues that are protected 2.3-fold above the intrinsic exchange rate. Thirty-seven residues could be followed at pD 6 and 27 residues at pD 7. Again no evidence for a significant super protected structure was observed. The properties of CTL9[11] are compared to other structured denatured states.

A detailed description of the denatured state is required for a complete characterization of the protein folding process. An understanding of the denatured state is also required to fully analyze protein stability studies because the measured stability reflects differences between the folded and unfolded ensemble, and unfolded state effects can be a significant factor. For example, point mutants in the *N*-terminal domain of L9 and RNase Sa have been shown to cause significant changes in stability by modulating denatured state properties (*1*, *2*). Unfolded state structure has also been shown to affect the thermodynamic properties of mesophilic and thermophilic variants of RNase H (*3*), whereas mutations in staphylococcus nuclease are believed to cause significant changes in the unfolded state ensemble (*4*−*6*). Residual structure in the denatured state can also play a significant role in protein refolding (*1*, *7*−*10*).

Denatured states are most easily studied at equilibrium, under conditions that drive protein unfolding, such as high concentration of denaturant, extremes of pH, or elevated temperatures. Although such studies can provide important clues about denatured state interactions (*8*, *11*−*14*), the denatured state populated under these conditions need not be equivalent to the denatured state under physiologically more relevant conditions (*15*, *16*). The denatured state that is most relevant to studies of folding and stability is that which is in equilibrium with the native state under native conditions. In a few special cases, it has been possible to study the denatured state under native-like conditions in the absence of a denaturant (*15*−*18*), but more generally, indirect approaches need to be applied.

In this article, we describe thermodynamic and amide H/D exchange studies that are designed to probe the denatured state of the *C*-terminal domain of the ribosomal protein L9 (CTL9). CTL9 is a small α-β protein that contains a mixed, parallel−antiparallel β-sheet with an unusual topology (Figure 1). The folding of the protein is two-state and is relatively slow over the pH range studied (pH 5 to 9) (*19*, *20*). The stability and folding kinetics of CTL9 are strongly coupled to pH, largely because the domain contains two buried histidines whose pK_a values are significantly lower in the folded state than those in the unfolded state (*19*, *20*). We have previously characterized the equilibrium unfolding of CTL9 in H_2O as a function of pH (*19*). Urea denaturations were conducted as a function of pH and used to determine $\Delta G°$ values in the absence of denaturants and *m* values, the dependence of $\Delta G°$ upon denaturant concentration. We found

† This work was supported by NIH Grant GM70941 to D.P.R.

* Corresponding author. Tel: 631-632-9547. Fax: 631-632-7960. E-mail: draleigh@notes.cc.sunysb.edu.

‡ Department of Chemistry.

§ Graduate Program in Biochemistry and Structural Biology.

|| Current address: Department of Biochemistry, University of Wisconsin at Madison, Madison, WI 53706.

[1] [1]Abbreviations: CD, circular dichroism; CTL9, *C*-terminal domain of ribosomal protein L9 from *Bacillus stearothermophilus*; $\Delta C_p°$, the change in heat capacity upon unfolding; $\Delta G_{ex}°$, the apparent free energy of the opening step in an amide H/D exchange experiment; $\Delta H°(T_m)$, the enthalpy of unfolding at T_m; GuHCl, guanidine hydrochloride; HSQC, heteronuclear single quantum correlation; NMR, nuclear magnetic resonance; T_m, the midpoint of the thermal unfolding transition; TOCSY, total correlation spectroscopy.

10.1021/bi052534o CCC: $33.50
Published on Web 06/24/2006

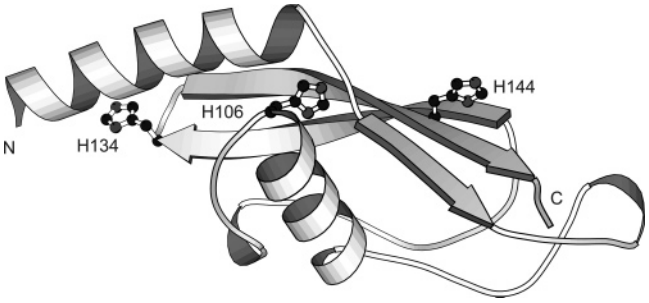

FIGURE 1: Ribbon diagram of CTL9 corresponding to residues 58−149 of L9. The Figure was made using the program MOLSCRIPT (*33*) and the pdb file 1DIV for the full length ribosomal protein L9. The *N*- and *C*-termini and the three histidines are labeled.

that the protein becomes less stable as the pH is lowered, but the *m* value increases significantly. The *m* values are related to the change in solvent accessible surface area between the folded and unfolded states (*11, 21*). Using NMR and CD, we have shown that the global fold of the protein does not change over the pH range studied; thus, these observations suggest an expansion of the unfolded state at lower pH. Here, we extended those studies by measuring the *m* values over a wider pH (pD) range and by measuring ΔC_p° as a function of pH. The ΔC_p° value of unfolding largely reflects changes in the exposure of polar and nonpolar surface areas between the folded and unfolded states (*21*). Thus, ΔC_p° should also be sensitive to changes in unfolded state structure (*22*). We compliment these studies with pH-dependent amide H/D exchange studies. Such experiments can provide information about the hydrogen-bonded structure in the unfolded state (*23*−*25*).

MATERIALS AND METHODS

Expression and Purification of Wild-Type and ^{15}N Uniformly Labeled CTL9. Wild-type CTL9 was expressed and purified as described previously (*19*). ^{15}N uniformly labeled protein was expressed in *E. coli* strain BL21(DE3) in 1 L of M9 minimal media with 0.8 g of ^{15}N-labeled NH_4Cl. Ampicillin was added to a final concentration of 100 mg/L. When the optical density (O. D.) at 600 nm reached about 0.7, protein expression was induced with the addition of IPTG (0.1 mM final concentration). The cells were harvested, and the protein was purified as previously described (*19*). The identity of the protein was confirmed by MALDI-TOF (matrix assisted laser desorption ionization time-of-flight mass spectrometry) with an expected molecular weight of 10 107 and an observed molecular weight of 10 098. The yield of the ^{15}N-labeled protein was about 5 mg/L.

Circular Dichroism (CD) Spectroscopy. All CD experiments were performed using Aviv Model 62A DS and 202SF circular dichroism spectrometers. Urea-induced unfolding and thermal unfolding measurements were performed in 20 mM phosphate and 100 mM NaCl buffers. The protein concentrations were 8−12 μM for all experiments. Both the denaturant-induced and thermal unfolding measurements were performed in a 1 cm quartz cuvette using a spectrometer bandwidth of 1.5 nm. Urea-induced denaturations were carried out using a titrator unit interfaced to the CD spectrometer. The signal at 222 nm was monitored for both urea-induced and thermal unfolding experiments. Reversibility was judged by the recovery of the signal at the conclusion of the experiment. The reversibility of thermal denaturations for CTL9 was more than 95% for both pH 5.45 and 8.0. Protein concentrations were determined from absorbance measurements at 276 nm in 6 M GuHCl at pH 6.5 using the extinction coefficient 1450 M^{-1} cm^{-1}.

Chemical and Thermal Denaturation Curve Fitting. Urea denaturation curves were fit using standard methods. Measurements were performed in both H_2O and D_2O. Deuterated urea was used for studies in D_2O. A two-state model was used to fit data collected from CD experiments to determine the stability, $\Delta G_u^\circ(H_2O)$, or $\Delta G_u^\circ(D_2O)$ in the absence of denaturant. CTL9 has previously been shown to follow two-state unfolding over the pH range 5 to 9 (*19*, *20*). The free energy of unfolding is assumed to be a linear function of denaturant concentration (*26*−*28*). The linear extrapolation model appears to be valid for CTL9 over the pH range studied (*19*).

$$\Delta G_U^\circ = \Delta G_u^\circ(H_2O) - m[\text{denaturant}] \quad (1)$$

where ΔG_u° is the apparent free energy for the N−D transition. The folded and unfolded baselines are assumed to be the linear function of the denaturant.

$$\theta_n([\text{urea}]) = a_n + b_n[\text{urea}] \quad (1a)$$

$$\theta_d([\text{urea}]) = a_d + b_d[\text{urea}] \quad (1b)$$

Thermal unfolding data were fit by assuming that the folded and unfolded baselines are linear functions of absolute temperature

$$\theta_n(T) = a_n + b_n T \quad (2a)$$

$$\theta_d(T) = a_d + b_d T \quad (2b)$$

The fraction denatured is given by

$$f_d = \frac{(\theta(T) - \theta_n(T))}{(\theta_d(T) - \theta_n(T))} \quad (3)$$

where $\theta(T)$ is the observed signal.

$$k_u = \frac{f_d}{f_n} = \frac{f_d}{(1 - f_d)} \quad (4)$$

k_u is the equilibrium constant for unfolding. The Gibbs−Helmholtz equation describes the temperature dependence of ΔG_u°

$$\Delta G_u^\circ(T) = \Delta H^\circ(T_m)(1 - T/T_m) - \Delta C_p^\circ((T_m - T) + T\ln(T/T_m)) \quad (5)$$

where $\Delta G_u^\circ(T)$ is the free energy of unfolding, T_m is the unfolding midpoint temperature, $\Delta H^\circ(T_m)$ is the enthalpy change at T_m, and ΔC_p° is the heat capacity change between the native and denatured states. Fits to individual thermal unfolding curves are insensitive to the initial value of ΔC_p°. The value of ΔC_p° was estimated to be about 1.0 kcal mol^{-1} deg^{-1} on the basis of the number of residues, and this value was used in the fits. Using the estimated ΔC_p° value, the T_m and $\Delta H^\circ(T_m)$ at each pH can be derived by fitting the individual thermal unfolding curve to the following equation

$$\theta(T) = \frac{((a_n + b_nT) + (a_d + b_dT)\exp(-\Delta G_u^\circ(T)/RT))}{(1 + \exp(-\Delta G_u^\circ(T)/RT))} \quad (6)$$

The values of $\Delta H^\circ(T_m)$ and T_m are insensitive to the exact choice of ΔC_p° and do not change if ΔC_p° is varied between 0.5 and 1.3 kcal mol^{-1} deg^{-1}. A precise value of ΔC_p° was determined by fitting temperature dependent ΔG_u° values to the Gibbs−Helmholtz equation.

Nuclear Magnetic Resonance (NMR) Studies. ^{15}N-coupled 3D HSQC-TOCSY experiments were carried out on a Bruker 700 MHz NMR spectrometer. Sensitivity enhanced pulse sequences were used. Assignments were obtained from 3D NMR experiments together with the assignments of the full-length L9 kindly provided by Professor David Hoffman.

Hydrogen−Deuterium exchange experiments were performed on a Varian INOVA 600 MHz instrument. A series of gradient sensitivity enhanced ^{15}N−^{1}H correlated heteronuclear single quantum coherence (HSQC) experiments were taken immediately after pure D_2O was added to the freeze-dried previously H_2O-exposed sample. Each spectrum required 20 min to collect. Eight scans per t1 value were collected, and the matrix size was 64 × 2048. The spectral width was 8000 Hz in the proton dimension and 2200 Hz in the ^{15}N dimension. The matrix was zero filled to 128 by 4096 points during processing. The experiments were performed at three pD values, 5.0, 6.0 and 7.0, using the exact same conditions and parameters. The pD values are the uncorrected pH meter reading in D_2O. A 20 mM deuterated acetate buffer was used, and the protein concentration was around 500 μM. All experiments were conducted at 25 °C.

Data Processing and Error Analyses of H/D Exchange Experiments. The volumes of the cross-peaks of the HSQC spectra were measured using FELIX 2000 software (Accelrys). Amide proton exchange rate constants were obtained by fitting peak volumes to a single first-order exponential decay versus time. At pD 5.0, the EX2 exchange mechanism is dominant ($k_{cl} \gg k_{in}$); thus, the expression for the exchange rate constant can be simplified to

$$k_{ex} = (k_{op}/k_{cl})\cdot k_{in} = K_u \cdot k_{in} \quad (7)$$

where k_{op} is the first-order rate constant for the opening step to form the exchange competent state, and k_{cl} is the first-order rate constant for the reverse reaction (closing step). The k_{cl} value corresponds to the refolding rate constants, k_f, for residues that exchange by global unfolding. The value of k_f was independently measured using stopped flow methods. For residues that exchange by global unfolding, k_{op} is given by k_u, the first-order rate constant for protein unfolding. The value of ΔG_{ex}° for the opening reaction was calculated using the measured exchange rate k_{ex} and the intrinsic exchange rate k_{in} determined by using the SPHERE program provided by the Roder laboratory (http://www.fccc.edu/research/labs/roder).

$$\Delta G_{ex}^\circ = -RT \ln(k_{ex}/k_{in}) \quad (8)$$

where R is the ideal gas constant, and T is the absolute temperature. The H/D exchange rates could be measured for one of the Histidines and the adjacent residue (H144, V145). For these residues, the intrinsic rates were corrected for pD effects by using the measured pK_a values to take into account the fraction ionized. Uncertainties in the apparent ΔG_{ex}° values were calculated by propagating the estimated uncertainties in the experimentally determined first-order rate constant k_{ex}

$$d\Delta G_{ex}^\circ = \pm RT\, dk_{ex}/k_{ex} \quad (9)$$

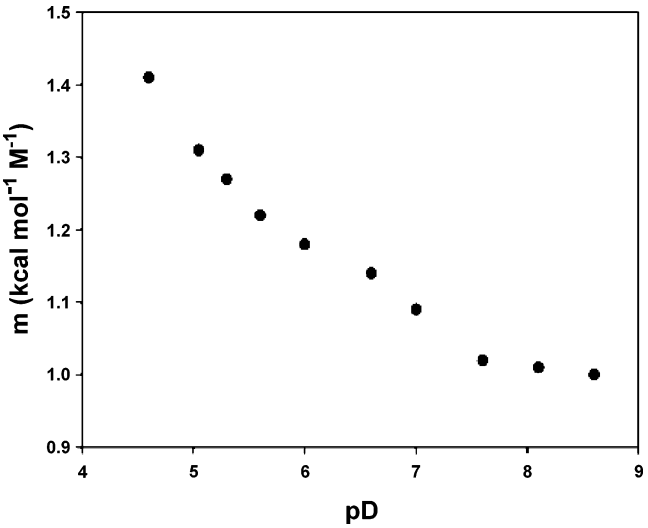

FIGURE 2: pD dependent *m* values of CTL9. The *m* values were derived from urea denaturation measurements. All measurements were conducted in D_2O containing 20 mM phosphate and 100 mM NaCl at 25 °C.

CTL9 contains three prolines, which are trans in the folded state. The ΔG° values determined by the H/D exchange were corrected for cis/trans isomerization in the unfolded state using the method of Pace (*29*). The correction is small, only about 0.15 kcal/mol.

At pD 6.0 and 7.0, the EX2 condition is not satisfied because the k_{cl} value for global unfolding (i.e., k_f) is no longer much greater than k_u; therefore, the full expression for the exchange rate is used to analyze the data as described in the results section. (The value of k_f (k_{cl}) was measured using stopped flow methods.)

RESULTS AND DISCUSSION

pH Dependent Thermodynamic Measurements Provide Evidence for Unfolded State Structure in CTL9. In anticipation of conducting H/D exchange measurements, we repeated our earlier stability measurements as a function of pD in D_2O. We also extended our measurements to cover a wider pD (pH) range, 4.75−8.25. The protein decreases in stability, but the *m* value increases. A plot of *m* versus pD is shown in Figure 2. The *m* value increases from 1.09 kcal mol^{-1} M^{-1} at pD 7.0 to 1.18 kcal mol^{-1} M^{-1} at pD 6.0, 1.32 kcal mol^{-1} M^{-1} at pD 5.0, and 1.41 kcal mol^{-1} M^{-1} at pD 4.75.

Similar to *m* values, the heat capacity change (ΔC_p°) between the unfolded state and the folded state also depends on the change in solvent accessible surface area; therefore, ΔC_p° should also depend on pH (*21*). Of course, other factors such as pH dependent changes in dynamics could also contribute. Thus, it is of interest to determine if ΔC_p° is pH dependent for CTL9 and if the pH dependence follows that observed for the *m* values. The classic method for determining ΔC_p° is to measure T_m and $\Delta H^\circ(T_m)$ as a function of

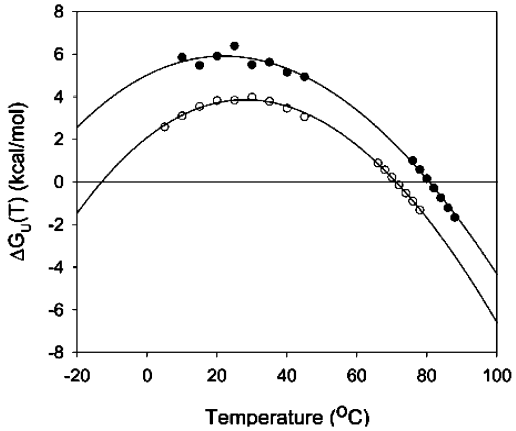

FIGURE 3: Gibbs−Helmholtz plot of the temperature dependence of the stability of CTL9 at pH 5.45 (○) and pH 8.0 (●). The unfolding free energy between 5 and 45 °C was obtained from urea denaturations. The points at higher temperatures were obtained from individual thermal unfolding curves. The solid lines are the best fit to the Gibbs−Helmholtz equation.

Table 1: Thermodynamic Parameters of CTL9 at pH 5.45 and 8.0[a]

	pH 5.45	pH 8.0
T_m (°C)	71.2	80.7
$\Delta H°(T_m)$ (kcal mol^{-1})[b]	60.3 ± 0.8	69.0 ± 2.4
$\Delta C_p°$ (kcal mol^{-1} deg^{-1})[b]	1.31 ± 0.03	1.07 ± 0.08
$\Delta G_u°$ (25°C) (kcal mol^{-1})[c]	3.82	5.77

[a]Data were derived from thermal unfolding and urea-induced unfolding measurements. All measurements were performed in H2O, 20 mM sodium phosphate, and 100 mM NaCl buffer. [b] $\Delta H°(T_m)$ and $\Delta C_p°$ values were obtained by fitting the temperature-dependent unfolding free energy curve obtained from the urea and thermal denaturations with the Gibbs−Helmholtz equation. [c] $\Delta G_u°$ at 25 °C was calculated from the above fit parameters.

pH. This approach cannot be used in our case because $\Delta C_p°$ is, itself, expected to be pH dependent. Instead, we used the Gibbs−Helmholtz equation to fit temperature dependent stability data. This approach has been successfully applied to a number of other proteins (*26*, *27*). The Gibbs−Helmholtz relationship indicates that T_m, $\Delta H°(T_m)$, and $\Delta C_p°$ are sufficient to describe the variation of $\Delta G°$ with temperature, provided that $\Delta C_p°$ is independent of temperature. $\Delta H°(T_m)$ and T_m can be reliably determined from the analysis of thermal unfolding curves, but $\Delta C_p°$ cannot normally be estimated from a single melting experiment. Here, we combine measurements of the unfolding free energy obtained from urea denaturations at different temperatures with a thermal unfolding experiment to estimate $\Delta C_p°$. The thermal unfolding experiment provides accurate estimates of $\Delta G°$ in the transition region. Together, these experiments measure $\Delta G°$ over a wide temperature range (5−88 °C in the present case). The data can be fit to the Gibbs−Helmholtz equation to obtain $\Delta C_p°$ and $\Delta H°(T_m)$. A plot of the temperature dependence of stability at pH 5.45 and 8.0 is shown in Figure 3, and the thermodynamic parameters are summarized in Table 1. The value of $\Delta C_p°$ increases from 1.07 kcal mol^{-1} deg^{-1} at pH 8.0 to 1.31 kcal mol^{-1} deg^{-1} at pH 5.45, about a 20% change in good agreement with the observed changes in *m* values over this range.

pH Dependent Amide H/D Exchange Measurements. Amide protection factors provide local probes of protein stability. They can also provide indirect but site specific information about the unfolded state structure (*24*, *25*, *30*).

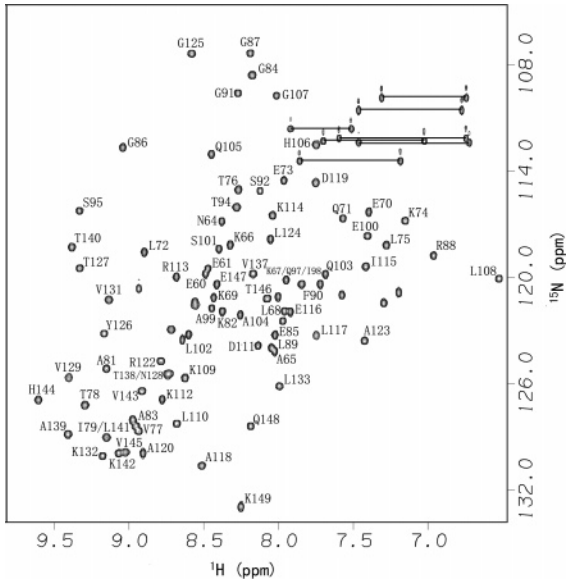

FIGURE 4: 2D ^{15}N−^{1}H correlated heteronuclear single quantum coherence (HSQC) spectrum of CTL9 enriched with ^{15}N in 90% H_2O/10% D_2O. The assignments of the backbone amide resonances, which are 98% complete, are labeled, and the pairs of amide resonances on side chains are connected by solid lines. The resonance of E136 is not in the region shown, and its chemical shift is 11.3 and 116.8 for the amide ^{1}H and ^{15}N, respectively.

Apparent $\Delta G°_{ex}$ values for the opening/exchange step can be calculated from the observed exchange rates and compared to the value of $\Delta G°$ for global unfolding, provided the exchange occurs in the EX2 limit. In this case, the observed rate of exchange is given by

$$k_{obs} = (k_{op}/k_{cl})k_{in} \quad (10)$$

where k_{op} is the rate of the opening reaction that leads to the exchange competent state, k_{cl} is the rate of the closing reaction, that is, the reverse reaction from the exchange competent state to the folded state, and k_{in} is the rate expected for a residue in an unstructured peptide of the same sequence. The ratio k_{op}/k_{cl} equals the equilibrium constant for unfolding, K_u, for those sites that exchange by complete unfolding. Additional protection beyond that expected for global unfolding provides evidence for unfolded state structure.

The exchange of the amide hydrogens was followed by recording a series of HSQC spectra after the protein was dissolved in D_2O. Each spectrum took about 20 min, and 20−40 spectra were collected, depending upon the pD used. The exchange rates were measured at pD 7.0, 6.0, and 5.0. These values were chosen because (1) they correspond to the pD range where there are significant changes in *m* value, and (2) the protein is stable enough to allow the exchange to be measured over this pD range. The assignments were determined by comparison to the assignments reported by the Hoffman group at pH 7.0 (*31*). A 3D ^{15}N-^{1}H HSQC−TOCSY experiment was recorded at pH 5.5 to confirm the low pH assignments. An example of the HSQC spectrum for CTL9 at pH 5.5 with the assignments is shown in Figure 4.

At pD 5.0, the peaks for 44 residues can be followed. The folding and unfolding rates of CTL9 have been determined as a function of pH (pD) (*20*). These data together with known intrinsic amide exchange rates allowed us to deter-

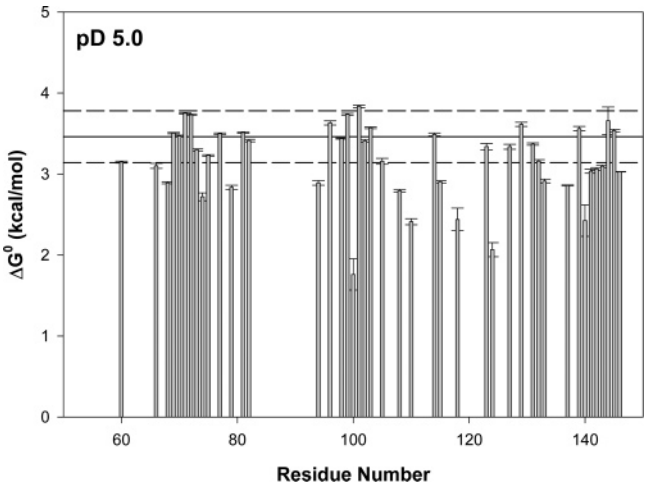

FIGURE 5: Plot of apparent free energies for the opening reaction calculated from the H/D exchange experiment at pD 5.0. The pD value is the uncorrected pH meter reading. The solid line represents the $\Delta G°$ values for each residue, and the dashed lines represent the range of $\Delta G°$ determined by urea denaturation in D_2O. The uncertainty in the urea denaturation measurements were estimated by performing the experiments in triplicate. Estimated uncertainties in the opening free energies range from 0.003 to 0.2 kcal mol^{-1}. The error bars are shown. All measurements were performed at 25 °C.

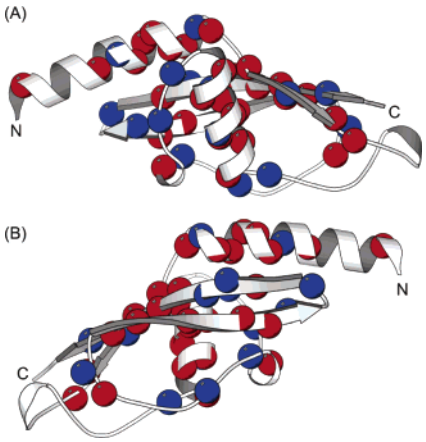

FIGURE 6: (A) Ribbon diagram of CTL9. Residues that exchange by global unfolding are shown as red spheres. The residues that exchange by subglobal unfolding are shown as blue spheres. (B) Diagram of CTL9 rotated by 180° around the *z* axis.

mine whether the EX2 limit is satisfied. The exchange satisfied the EX2 limit under these conditions (Materials and Methods). In this case, the observed rate of exchange can be combined with the intrinsic rate of exchange expected for an unstructured polypeptide of the same sequence to calculate the free energy for opening step, the conformational transition to the exchange competent state ($\Delta G_{ex}°$). The value of $\Delta G_{ex}°$ will be given by $\Delta G_U°$ for sites that exchange by complete unfolding. A plot of calculated $\Delta G°_{ex}$ versus the residue is shown in Figure 5. Twenty-nine of the 44 residues that could be followed exchange with a free energy of opening consistent with global unfolding. The others exchanged with rates faster than those expected for global unfolding. These sites exchange by subglobal unfolding. A ribbon diagram of the protein is shown in Figure 6, with the residues that exchange via global unfolding indicated as red spheres. The 29 residues are scattered throughout the structure. All of the sites that exchange by global unfolding are involved in hydrogen bonds. The unfolding free energy estimated by urea denaturation in D_2O is 3.46 kcal mol^{-1} with an upper limit of 3.78 kcal mol^{-1}. A few sites had opening free energies larger than 3.46 kcal mol^{-1}, but no resonances had a free energy for opening above the range of the global unfolding free energy. Thus, there is no direct evidence for significantly persistent hydrogen-bonded secondary structure in the unfolded state ensemble.

Given the estimated uncertainty in our urea denaturation experiments, a site would have to have a $\Delta G_{op}°$ value 0.5 kcal mol^{-1} greater than the $\Delta G_U°$ value to be classified as superprotected. This corresponds to a 2.3-fold decrease in the exchange rate in the unfolded state relative to k_{in}, that is, given the limits of precision of our stability measurements, we can only detect sites whose unfolded state exchange rates are 2.3 times slower than those predicted by their intrinsic rates. It is of course possible that some sites experience partial protection in the unfolded state, that is, less than our detection limit. Shortle and co-workers have argued that protection factors of less than five in the denatured proteins are likely unreliable (*30*).

At higher pD values, 6.0 and 7.0, the EX2 exchange condition is no longer satisfied. In this case, exchange must be analyzed using the full expression for the observed rate (*23*).

$$k_{ex} = k_{op} \cdot k_{in}/(k_{cl} + k_{in}) \qquad (11)$$

where $k_{op} = k_u$ and $k_{cl} = k_f$ for sites that exchange via global unfolding. In general, it is not possible to directly calculate the opening free energy from exchange data collected at one pH because the expression for k_{obs} contains two unknowns, k_{op} and k_{cl}. In favorable cases, one can globally fit pH dependent data assuming that k_f and k_u are independent of pH. This is not applicable to CTL9 because stability and folding kinetics are strongly pH dependent. Consequently, we adopted another approach to analyze the exchange data. CTL9 is a two-state folder, and accurate measurements of the rate constant for global refolding k_f can be determined via pH or urea jump-stopped-flow studies (*19*). The value of k_u can be derived from k_f and $\Delta G°$. The expected exchange rate of each residue can, thus, be calculated for residues that exchanged by global unfolding. The difference between the calculated and the observed k_{ex} pinpoints the residue(s) that exchanged more rapidly than the global unfolding residues, thus indicating those sites that exchange by subglobal unfolding. Plots of the difference between the observed exchange rate constant and the rate constant expected for global unfolding for each residue were generated (Figure 7). Thirty-seven residues could be followed at pD 6.0 and 27 residues at pD 7.0. Twenty-five residues at pD 6 and 19 residues at pD 7 exchange by global unfolding. Because of the analysis employed, it is difficult to precisely define the range of rates that fall within the global folding category. Hence, these numbers are estimated. The decrease in the number of residues that exchange by global unfolding at pD 7 relative to pD 6 does not necessarily imply that the slow dynamics of the protein has changed. It may just reflect the increased stability at pD 7 relative to that at pD 6. The analysis also allows the detection of residues that exhibit super protection, that is, those sites that exchange more slowly than that expected from global unfolding. Such sites

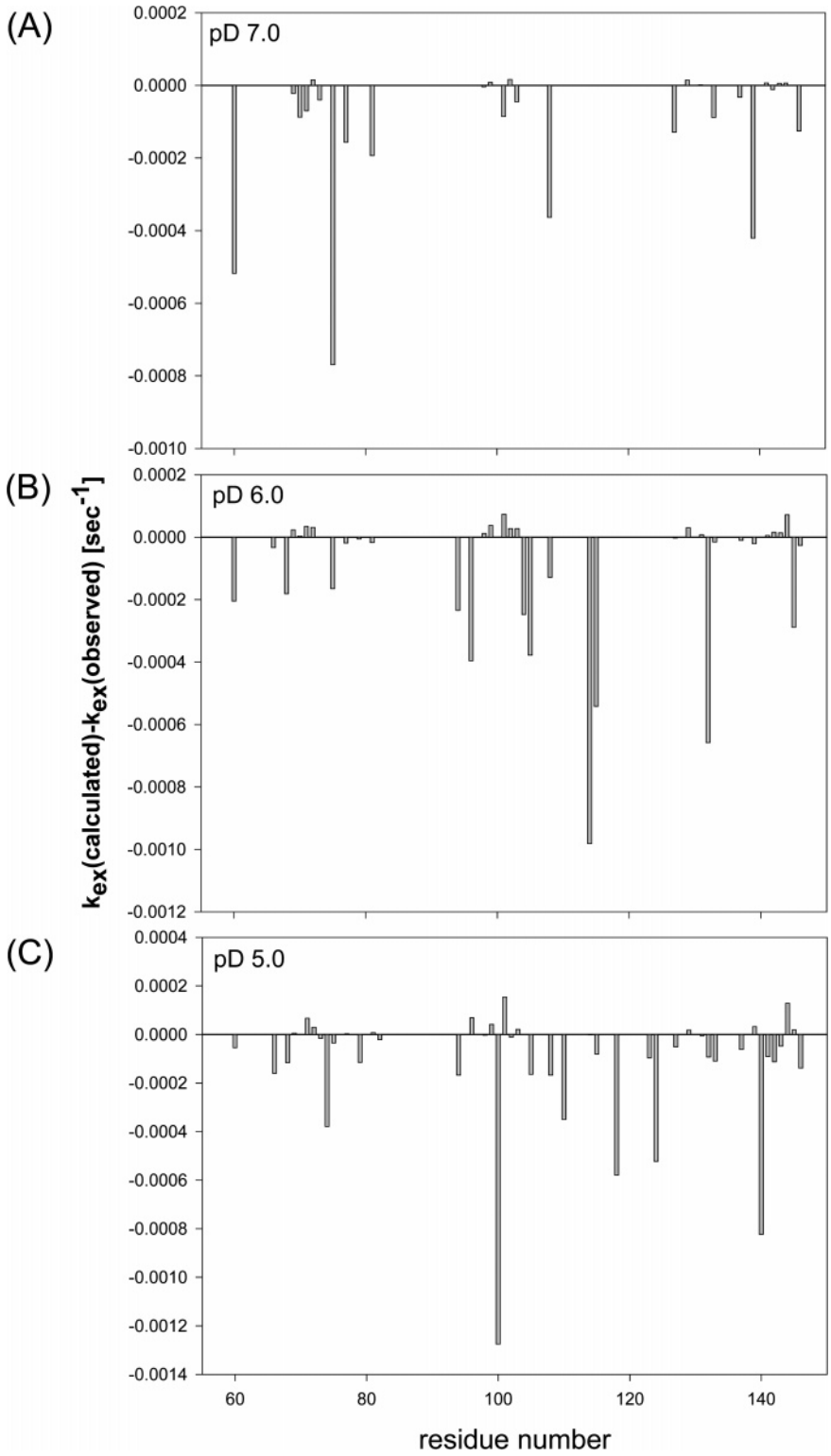

FIGURE 7: Plots of the deviation between the observed exchange rate constants from H/D exchange experiments and those calculated assuming that exchange occurs by global unfolding. (A) pD 7.0; (B) pD 6.0; and (C) pD 5.0. All pD values are uncorrected pH meter readings. The bars above zero represent the residues that exchange more slowly than that predicted by global unfolding, and the bars below zero represent the residues that exchange faster than that predicted by global unfolding. All measurements were performed at 25 °C.

likely take part in hydrogen-bonded structure in the unfolded state. No significant highly protected residues were found at either pD values.

CONCLUSIONS

Our thermodynamic analysis provides good evidence for pH dependent interactions in the unfolded state of CTL9. The increase in ΔC_p° as the pH is lowered parallels the measured increase in the *m* value. These observations suggest a pH dependent expansion of the unfolded state with the unfolded state becoming more expanded at lower pH. The most plausible explanation for this behavior is that protonation of the histidines leads to a charge-induced expansion of the unfolded state, presumably by causing the disruption

of hydrophobic clusters. pH dependent stability measurements on a set of His to Gln point mutants of CTL9 indicate that the unfolded state pK_a values of the histidines are not strongly perturbed from random coil models. A global analysis of the data indicates that the simplest self-consistent model is one in which each histidine has an unfolded state pK_a close to 6.8 (*20*). If correct, this would rationalize the significant increase in the *m* value and $\Delta C_p°$ observed below pD 7.5. The predicted net charge of the unfolded protein is +4.1 at pH 7.4, increasing to +7.3 at pH 5.6, calculated using pK_a values corresponding to isolated residue values. The increase in charge is consistent with a model that invokes charge-induced expansion. Interestingly, the *m* value still increases below pD 5, suggesting that additional residues might be taking part. The most likely candidates are obviously Asp or Glu. The calculated net charge of the unfolded state continues to increase as the pH is decreased below 5.6, reaching a value of +9.1 at pH 5.0 and +14.4 at pH 4.1. pH dependent hydrophobic clusters in the unfolded state have been proposed to play a role in other systems, notably in RNase Sa, Barnase, s. nuclease, and ribonuclease H (*2*, *3*, *6*, *32*).

The thermodynamic measurements provide indirect probes of interactions that lead to compact denatured states, but they do not offer residue specific information or much insight into potential hydrogen bonded structure. For that we turned to amide H/D exchange studies. At the lowest pD probed, pD 5.0, we found no evidence for any residues exhibiting so-called super protection. This argues against significantly persistent hydrogen-bonded structure in the unfolded state. The data collected at pD 5.0 was easily analyzed because the exchange fell within the EX2 limit. At the higher pD values, this was no longer the case, and the complete expression for exchange needed to be considered. Our approach is somewhat novel in that we determined k_f and k_u by stopped flow methods in conjunction with equilibrium stability. With these values in hand, we could calculate the expected exchange rate for residues that exchange by complete global unfolding. This allows us to detect sites that exhibit super protection. Again, no super protected sites were detected at either pD 6 or 7, arguing against persistent hydrogen-bonded structure in the unfolded state under these conditions. Of course, the studies are limited by the precision of the measurements and would not be able to detect sites whose protection factors were moderately increased over those expected for an unstructured peptide. At pD 5.0, the estimated precision of the experiments limits detection to residues that have protection factors of 2.3 or greater. Thus, it is important to stress that the exchange studies do not imply the complete absence of hydrogen bonding interactions in the unfolded state and should certainly not be interpreted to mean that the unfolded state lacks any residual structure. Along these lines, Shortle and co-workers have pointed out that a partially formed helical structure should provide only very low protection factors. Following their argument, consider the case where a helix is fully formed 30% of the time and unstructured 70% of the time. The overall protection factor for exchange will still be very low (1.43), even if the H-bonded residues in the helical state have infinite protection factors (*30*). In fact, studies of the unfolded state at pH 4.0 indicate that there is a residual CD signal that differs from what is expected for a random coil (*15*). The picture that emerges from these studies is that the unfolded state of CTL9 contains significant interactions presumably hydrophobic in nature that lead to compaction but are not sufficient to confer significant protection to hydrogen bonds. The unfolded state of CTL9 appears to be very similar to the Δ131Δ fragment of s. nuclease (*30*) in that it is compact and contains residual structure yet lacks protected amides. Thus, this may be a general feature of unfolded states.

ACKNOWLEDGMENT

We thank Dr. Martine Ziliox and Mr. Francis Picart for assistance with 3D NMR experiments.

SUPPORTING INFORMATION AVAILABLE

The assignments of the NMR resonances of CTL9 at pH 5.5 and the apparent exchange rate constants at pD 7.0, 6.0, and 5.0.

REFERENCES

1. Cho, J. H., Sato, S., and Raleigh, D. P. (2004) Thermodynamics and kinetics of non-native interactions in protein folding: a single point mutant significantly stabilizes the N-terminal domain of L9 by modulating non-native interactions in the denatured state, *J. Mol. Biol. 338*, 827−837.
2. Pace, C. N., Alston, R. W., and Shaw, K. L. (2000) Charge-charge interactions influence the denatured state ensemble and contribute to protein stability, *Protein Sci. 9*, 1395−1398.
3. Robic, S., Guzman-Casado, M., Sanchez-Ruiz, J. M., and Marqusee, S. (2003) Role of residual structure in the unfolded state of a thermophilic protein, *Proc. Natl. Acad. Sci. U.S.A. 100*, 11345−11349.
4. Shortle, D. (2002) The expanded denatured state: an ensemble of conformations trapped in a locally encoded topological space, *Adv. Protein Chem. 62*, 1−23.
5. Shortle, D. (1996) The denatured state (the other half of the folding equation) and its role in protein stability, *FASEB J. 10*, 27−34.
6. Whitten, S. T., and Garcia-Moreno, E. B. (2000) pH dependence of stability of staphylococcal nuclease: evidence of substantial electrostatic interactions in the denatured state, *Biochemistry 39*, 14292−14304.
7. Myers, J. K., and Oas, T. G. (2001) Preorganized secondary structure as an important determinant of fast protein folding, *Nat. Struct. Biol. 8*, 552−558.
8. Yao, J., Chung, J., Eliezer, D., Wright, P. E., and Dyson, H. J. (2001) NMR structural and dynamic characterization of the acid-unfolded state of apomyoglobin provides insights into the early events in protein folding, *Biochemistry 40*, 3561−3571.
9. Jemth, P., Gianni, S., Day, R., Li, B., Johnson, C. M., Daggett, V., and Fersht, A. R. (2004) Demonstration of a low-energy on-pathway intermediate in a fast-folding protein by kinetics, protein engineering, and simulation, *Proc. Natl. Acad. Sci. U.S.A. 101*, 6450−6455.
10. Trefethen, J. M., Pace, C. N., Scholtz, J. M., and Brems, D. N. (2005) Charge-charge interactions in the denatured state influence the folding kinetics of ribonuclease Sa, *Protein Sci. 14*, 1934−1938.
11. Tanford, C. (1968) Protein denaturation, *Adv. Protein Chem. 23*, 121−282.
12. Logan, T. M., Theriault, Y., and Fesik, S. W. (1994) Structural characterization of the FK506 binding protein unfolded in urea and guanidine hydrochloride, *J. Mol. Biol. 236*, 637−648.
13. Neri, D., Billeter, M., Wider, G., and Wuthrich, K. (1992) NMR determination of residual structure in a urea-denatured protein, the 434-repressor, *Science 257*, 1559−1563.
14. Klein-Seetharaman, J., Oikawa, M., Grimshaw, S. B., Wirmer, J., Duchardt, E., Ueda, T., Imoto, T., Smith, L. J., Dobson, C. M., and Schwalbe, H. (2002) Long-range interactions within a nonnative protein, *Science 295*, 1719−1722.
15. Li, Y., Picart, F., and Raleigh, D. P. (2005) Direct characterization of the folded, unfolded and urea-denatured states of the C-terminal domain of the ribosomal protein L9, *J. Mol. Biol. 349*, 839−846.

16. Zhang, O., and Forman-Kay, J. D. (1995) Structural characterization of folded and unfolded states of an SH3 domain in equilibrium in aqueous buffer, *Biochemistry 34*, 6784−6794.
17. Tollinger, M., Kay, L. E., and Forman-Kay, J. D. (2005) Measuring p*K*(a) values in protein folding transition state ensembles by NMR spectroscopy, *J. Am. Chem. Soc. 127*, 8904−8905.
18. Tang, Y., Rigotti, D. J., Fairman, R., and Raleigh, D. P. (2004) Peptide models provide evidence for significant structure in the denatured state of a rapidly folding protein: the villin headpiece subdomain, *Biochemistry 43*, 3264−3272.
19. Sato, S., and Raleigh, D. P. (2002) pH-dependent stability and folding kinetics of a protein with an unusual alpha-beta topology: the C-terminal domain of the ribosomal protein L9, *J. Mol. Biol. 318*, 571−582.
20. Horng, J. C., Cho, J. H., and Raleigh, D. P. (2005) Analysis of the pH-dependent folding and stability of histidine point mutants allows characterization of the denatured state and transition state for protein folding, *J. Mol. Biol. 345*, 163−173.
21. Myers, J. K., Pace, C. N., and Scholtz, J. M. (1995) Denaturant m values and heat capacity changes: relation to changes in accessible surface areas of protein unfolding, *Protein Sci. 4*, 2138−2148.
22. Privalov, P. L., Tiktopulo, E. I., Venyaminov, S. Yu., Griko, Yu. V., Makhatadze, G. I., and Khechinashvili, N. N. (1989) Heat capacity and conformation of proteins in the denatured state, *J. Mol. Biol. 205*, 737−750.
23. Englander, S. W., and Mayne, L. (1992) Protein folding studied using hydrogen-exchange labeling and two-dimensional NMR, *Annu. Rev. Biophys. Biomol. Struct. 21*, 243−265.
24. Rohl, C. A., Scholtz, J. M., York, E. J., Stewart, J. M., and Baldwin, R. L. (1992) Kinetics of amide proton exchange in helical peptides of varying chain lengths. Interpretation by the Lifson−Roig equation, *Biochemistry 31*, 1263−1269.
25. Marmorino, J. L., Auld, D., Betz, S. F., Doyle, D. F., Young, G. B., and Pielak G. J. (1993) Amide proton exchange rates of oxidized and reduced *Saccharomyces cerevisiae* iso-1-cytochrome *c*, *Protein Sci. 2*, 1966−1974.
26. Nicholson, E. M., and Scholtz, J. M. (1996) Conformational stability of the *Escherichia coli* HPr protein: Test of the linear extrapolation method and a thermodynamic characterization of cold denaturation, *Biochemistry 35*, 11369−11378.
27. Agashe, V. R., and Udgaonkar, J. B. (1995) Thermodynamics of denaturation of barstar: Evidence for cold denaturation and evidence of the interaction with guanidine hydrochloride, *Biochemistry 34*, 3286−3299.
28. Santoro, M. M., and Bolen, D. W. (1988) Unfolding free energy changes determined by the linear extrapolation method. 1. Unfolding of phenylmethanesulfonyl α-chymotrypsin using different denaturants, *Biochemistry 27*, 8063−8068.
29. Huyghues-Despointes, B. M., Scholtz, J. M., and Pace, C. N. (1999) Protein conformational stabilities can be determined from hydrogen exchange rates, *Nat. Struct. Biol. 6*, 910−912.
30. Mori, S., van Zijl, P. C., and Shortle, D. (1997) Measurement of water-amide proton exchange rates in the denatured state of staphylococcal nuclease by a magnetization transfer technique, *Proteins 28*, 325−332.
31. Hoffman, D. W., Cameron, C. S., Davies, C., White, S. W., and Ramakrishnan, V. (1996) Ribosomal protein L9: a structure determination by the combined use of X-ray crystallography and NMR spectroscopy, *J. Mol. Biol. 264*, 1058−1071.
32. Pace, C. N., Laurents, D. V., and Erickson, R. E. (1992) Urea denaturation of barnase: pH dependence and characterization of the unfolded state, *Biochemistry 31*, 2728−2734.
33. Kraulis, P. J. (1991) MOLSCRIPT: a program to produce both detailed and schematic plots of protein structures, *J. Appl. Crystallogr. 24*, 946−950.

BI052534O